metals

MDPI

Article

Influence of Alkyd Composite Coatings with Polyaniline Doped with Different Organic Acids on the Corrosion of Mild Steel

Branimir N. Grgur *, Aleksandra S. Popović and Ayad Salem §

Faculty of Technology and Metallurgy, University of Belgrade, Karnegijeva 4, 11020 Belgrade, Serbia; apopovic@tmf.bg.ac.rs

* Correspondence: bngrgur@tmf.bg.ac.rs

§ In the memory of Ayad, 1965–2022.

Abstract: Composite coatings prepared by mixing 5 wt.% polyaniline with commercial alkyd-based paints were applied on carbon steel. The polyaniline emeraldine chloride salt was prepared by procedure recommended by IUPAC, including deprotonation by ammonia hydroxide, and reprotonation with sulfamic, succinic, citric, and acetic acids with different doping degrees or oxidation states. The steel samples with base and composite coatings were immersed in 3% NaCl and the corrosion current density was determined after 96 h in situ using the ASTM 1,10-phenanthroline method. The samples were also inspected by optical microscopy. It was shown that the composite coatings reduced the possibility of blister formations and delamination. The corrosion current density and the appearance of the corrosion products, whose area was determined by ImageJ software, closely followed the initial oxidation state of the polyaniline. It was also shown that damaged composite coatings with higher degrees of oxidized (doped) polyaniline were more prone to formation of corrosion products. The role of the initial state of the polyaniline is discussed. It is suggested that such behavior could be connected to the oxygen reduction reaction mechanism that proceeds mainly via two electron paths on the polyaniline particles, releasing a much smaller amount of hydroxyl ions, which is responsible for the delamination and blister formation of the commercial coatings.

Keywords: phenanthroline method; reprotonation; delamination; blistering; protection mechanism

Citation: Grgur, B.N.; Popović, A.S.; Salem, A. Influence of Alkyd Composite Coatings with Polyaniline Doped with Different Organic Acids on the Corrosion of Mild Steel. *Metals* **2023**, *13*, 1364. https://doi.org/10.3390/met13081364

Academic Editor: Dake Xu

Received: 7 June 2023
Revised: 30 June 2023
Accepted: 6 July 2023
Published: 29 July 2023

1. Introduction

Mild steels due to their good mechanical characteristics, low price, etc., are common construction materials in many industries and different applications. Unfortunately, it has low corrosion stability and is easily corroded in many different environments [1,2]. Consequently, mild steel must be protected against corrosion, and one of the most common methods is the application of different organic coatings [3]. But over time, the coatings protective characteristics decay; thus, many researchers have investigated different additives to prolong the protective ability including different conducting polymers with the main focus on polyaniline [4].

Polyaniline (PANI), due to its easy chemical or electrochemical synthesis, inexpensive monomer, distinct electrical, redox, and acid–base characteristics in addition to its various potential uses in many technical areas, like supercapacitors, sensors, antimagnetic shielding, antistatic coatings, etc., has been the subject of considerable research in the past [5,6]. Among the other applications, there was a lot of effort made in the field of corrosion protection of metals and alloys. The main focus has been on steel [7–9] and some other metals, like aluminum [10], magnesium alloys [11,12], copper [13], etc.

Two basic polyaniline forms, the polyaniline emeraldine salt form (PANI-ES) and the polyaniline emeraldine base form (PANI-EB), are being investigated for their use as

additives to anti-corrosion composite coatings. Some studies have confirmed the non-conducting nature of PANI-EB and its barrier effect; however, some researchers found that PANI-ES had an anodic protective or inhibitory effect, while others found inconclusive results [7,14–17]. The composite organic coatings containing different forms of PANI are widely investigated in the corrosion protection of metals [7,18], but the mechanism of the corrosion protection of mild steel is still elusive [7,19]. More information can be found in [9] and the references therein. Accordingly, it is crucial to keep researching the different forms of composite PANI-based coatings on steel to resolve the mechanism and the role of polyaniline in the evident corrosion protection ability.

In our previous paper [20], a PANI composite with an alkyd-based paint prepared with PANI possessing different initial oxidation states and doped with organic acids was qualitatively investigated using the linear polarization methods. It was observed that the polarization resistance decreased with a decrease in the initial oxidation state of the polyaniline. Also, paint blistering and delamination were suppressed to a large extent in comparison with the base coating. Consequently, to extend that work, in this paper, we present the results of the quantitatively determined corrosion current densities using the 1,10-phenanthroline standard test method that is already used for corrosion current determination of composite coatings containing polyaniline doped with benzoate [21]. We also determined the corrosion product area on the base and composite coating surfaces. Also, a plausible mechanism of corrosion protection will be discussed in more detail. The possible applications of composite coating are also suggested.

2. Materials and Methods

As already described in our previous work [20], polyaniline in a powdered form was produced using the chemical synthesis route suggested by the International Union of Pure and Applied Chemistry (IUPAC) guidelines [22]. In the procedure, 0.22 mol of aniline monomer (20.5 g or 20.8 cm^3, p.a. Sigma-Aldrich, St. Louis, MO, USA) previously distilled under low-pressure conditions) and 0.22 mol of HCl (8 g or 26 cm^3 of 37 wt.% HCl, p.a. Merck) were mixed at ambient temperature in 500 mL of distilled water to produce anilinium hydrochloride. Following vigorous stirring, 500 mL of 0.22 mol HCl containing 0.275 mol (62.81 g) of ammonium persulfate, $(NH_4)_2S_2O_7$, was slowly added. After 24 h of mixing with a magnetic stirrer, the obtained green powder was filtered, repeatedly washed with 0.1 M HCl, distilled water, and acetone, and then finally dried for 24 h in an oven at 60 °C. To form the polyaniline emeraldine base (PANI-EB), a portion of the as-synthesized polyaniline emeraldine salt powder (PANI-ES) was added to 1 M NH_4OH, and deprotonated during 24 h under stirring conditions. The reported electrical conductivity of PANI-ES prepared by using the recommended IUPAC procedure is 4.4 ± 1.7 S cm^{-1} (average of 59 samples) and the PANI-EB electrical conductivity should be 3×10^{-9} S cm^{-1} [22]. The resulting polyaniline emeraldine base powder was added to the solutions containing either 0.87 M sulfamic, 1 M succinic, 1 M citric, or 1 M acetic acid in order to produce the reprotonated polyaniline, through the route described by Stejskal et al. [23]. Typically, 100 cm^3 solutions of the mentioned acids are continuously mixed for 24 h with 2 g of the PANI-EB, and after that, the solutions were filtered, rinsed with distilled water and acetone, and dried for 48 h. Scheme 1 illustrates the reprotonotation of the polyaniline emeraldine base to the emeraldine salt form using acids (HA), while Table 1 presents the characteristics of the physical–chemical data of the acids used for polyaniline reprotonation.

The UV-vis spectra of all PANI samples in a powdered form dispersed in distilled water (~15 mg in 20 cm^3) were obtained using LLG uniSPEC 2 spectrophotometers (Lab Logistics Group, Meckenheim, Germany). The water dispersions of the polyaniline were prepared by vigorous sonication for 0.5 h, and then allowing for the precipitation of larger particles for 1 h.

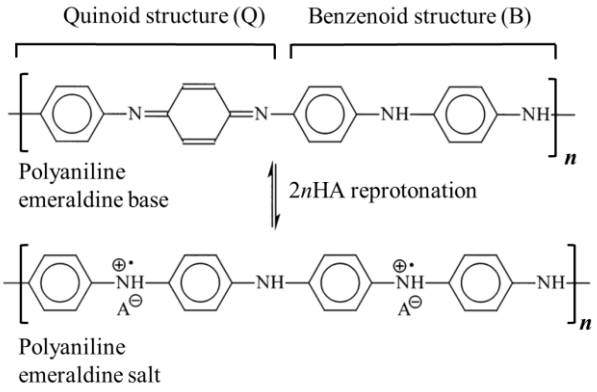

Scheme 1. The reprotonotation of the polyaniline emeraldine base to emeraldine salt form. HA: organic acid.

Table 1. The characteristics data of the acids used and their concentrations, $c_{HA,}$ used for the reprotonation of the polyaniline base form, and σ is the reported conductivity of the reprotonated samples "data from [23]".

Acid	Structure	M_w g mol^{-1}	pK_a	c_{HA} M	pH	σ S cm^{-1}
Acetic	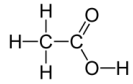	60.1	4.76	1	2.6	7.1×10^{-9}
Succinic	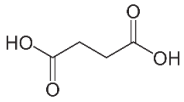	118.1	pK_{a1} = 4.2 pK_{a2} = 5.6	0.87 (sat)	2.5	5.9×10^{-6}
Citric	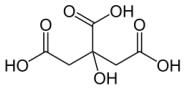	192.1	pKa_1 = 3.13 pKa_2 = 4.76	1	1.51	4.4×10^{-3}
Sulfamic	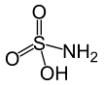	97.1	1.0	1	0.6	0.11

The composite coatings containing reprotonated PANI were prepared using the commercial white finishing paint for steel "*Professional emajl lak*" (Nevena Color Xemmax, Leskovac, Serbia), which contains an alkyd binder and white pigments in organic thinners (67% solids). The mass of the solids was determined by measuring the mass of wet and dry paint. The composite coating was prepared by mixing 10 g of the base paint with 5 wt.% of well-ground reprotonated PANI powder, 0.33 g of dry paint, with a particle size in the range of 0.5 to 1.0 μm that was separated from the PANI powder using corresponding sieves. The base and composite coatings were applied using a paint roller on the properly prepared samples of low-carbon, ≤0.13 C, mild steel (ANSI 1212) with dimensions of 4.5 cm × 5 cm and an exposed area of 22.5 cm^2. The backsides and the edges of the steel samples were isolated with an approximately 200 μm thick epoxy coating. After proper drying at room temperature for 48 h, the average coating thickness of 25 μm was measured using a Byko-test 4500 FE/NFe (BYK-Gardner, Wesel, Germany) thickness tester. The samples were immersed in five laboratory glass beakers with a volume of 200 cm^3 containing 3% NaCl solution. The same procedure was used to prepare the samples for the investigations of self-healing properties but on mild steel with dimensions of 2 cm × 5 cm, on which the cross was engraved with a sharp awl. The samples were immersed in five glass beakers with a volume of 200 cm^3 containing a 3% NaCl solution. The corrosion properties were estimated according to the visual observations.

The average corrosion current density of the mild steel samples painted with the base and composite coatings, as the mass of iron in a beaker with a volume of 200 cm^3 of

3% NaCl solution, was determined after 96 h of corrosion using the ASTM International 1,10-phenanthroline standard method [24]. 1,10-phenanthroline reacts with ferrous ions generating an intensely red-colored complex. In a typical route, after 96 h of corrosion and the first corrosion product on the samples was observed, 10 cm^3 of the stock solutions was added to 100 cm^3 volumetric flasks containing 0.25 cm^3 of concentrated sulfuric acid and 20 cm^3 of distilled water. Then, 1 cm^3 of the hydroxylamine solution, with a concentration of 100 g dm^3, 10 cm^3 of the 1,10-phenanthroline solution, with a concentration of 1 g dm^{-3}, and 8 cm^3 of the 1.2 M sodium acetate solution, were added and distilled water was added up to a final volume of 100 cm^3. The mass of the iron in the corrosive solutions was determined 96 h after the immersion of the samples in the corrosive media by recording the UV–visible spectra using a LLG uniSPEC 2 spectrophotometer and determining the value of the absorbance at 508 nm of the investigated solutions and using the calibration line of the standard solution. The samples were left to corrode for a total of 150 h, and the corroded area was determined from the sample images using ImageJ software [25]. For the preparation of the iron standard test solutions and determination of the calibration line from the UV–visible spectra, the appropriate amounts of ferrous ammonium sulfate hexahydrate, $Fe(NH_4)_2(SO_4)_2 \times 6H_2O$ (Sigma-Aldrich, St. Louis, MO, USA), were used (1.000 g contains 0.1443 g of iron). The iron standard solution was prepared by dissolving 0.7022 g of ferrous ammonium sulfate hexahydrate in 500 cm^3 of distilled water containing 20 cm^3 of concentrated sulfuric acid and diluting it to 1000 cm^3 with distilled water. A volume of 100 cm^3 of this solution was then diluted to 1000 cm^3. For the determination of the calibration curve, an adequate volume of the standard solutions was used to prepare 100 cm^3 of the Fe^{2+} solution in the range of 18.6 µg to 186 µg of Fe^{2+}.

The optical micrographs were acquired using an optical microscope (Olympus CX41, Olympus, Tokyo, Japan) equipped with a digital camera and connected to a PC. The image of the whole samples was obtained using a PANASONIC DC-FZ82 digital camera (Panasonic Corporation, Kadoma, Osaka, Japan).

3. Results

3.1. Characterization of the Samples

The UV–visible spectra of the PANI samples that had been sonicated in distilled water in the range of the wavelengths from ~200 to 1100 nm are presented in Figure 1. The as-synthesized PANI in the emeraldine salt form (PANI-ES) had an absorption peak at 365 nm that is connected to the π–π* transition inside the benzenoid ring (B). The peak at 440 nm can be connected to the polaron–π* transition inside the quinoid structure (Q), followed by a broad tail associated with polaronic structures [26,27]. The spectrum of PANI in the emeraldine base form (PANI-EB) around the peak at ~365 nm had a strong broad peak with maximum absorbance at ~700 nm that is ascribed to the molecular excitation connected with the quinoid–imine structure [27]. As shown by few research [28–32] the ratio of absorbance of quinoid (polaron–π* transition) to benzenoid (π–π* transition) can be used to estimate PANI oxidation degree. In our case the ratio of absorbance for PANI-ES of quinoid (polaron–π* transition at 440 nm) to benzenoid (π–π* transition at 365 nm), denoted as $A_{440}/_{365}$, can be taken as a measure of the oxidation state of the PANI conducting polymer [27–31]. All four reprotonated samples had a well-defined absorption maximum at 365 nm from the π–π* transition inside the benzenoid ring. The polyaniline doped with sulfamic acid had a shoulder at 440 nm from the polaron—π* transition, while the other three samples had an increased absorbance.

Figure 2 shows the particle size distribution in the composite coating of the polyaniline doped with sulfamic acid (shown in the inset of Figure 2) determined using ImageJ software. It can be seen that main particle sizes were approximately 13 µm, while some agglomerates had much higher dimensions, from approximately 20 µm up to 110 µm. The high agglomeration tendency of PANI is affected by the inflexibility in the conjugated double-bond backbone and is caused by the high density of electrical charges inside the conducting polymer matrix [33]. Consequently, it is difficult to make a proper dispersion of

PANI in the classical organic polymer paint which is one of the main issues for possible applications.

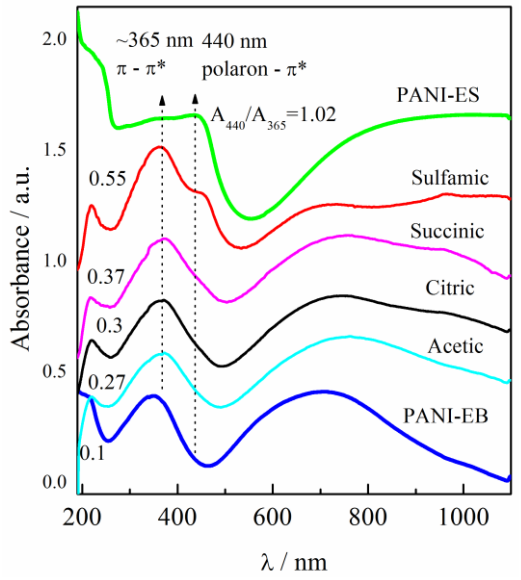

Figure 1. UV-vis spectra of polyaniline salt (PANI-ES) and base (PANI-EB) water dispersions synthesized according to the IUPAC recommendations, in comparison with PANI-EB samples reprotonated with different organic acids (marked in the figure). Reproduced from [20] with permission from Elsevier B.V., 2018.

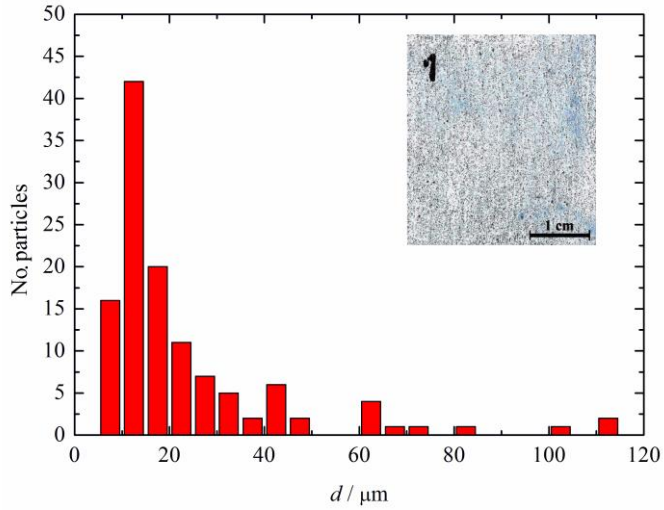

Figure 2. The particle size distribution of the polyaniline doped with sulfamic acid in the composite coating shown in the inset.

3.2. Corrosion Behavior

The UV–visible spectra of the standard test solutions are shown in Figure 3a. The linear dependence of the absorption of the standard solutions at 508 nm, shown in the inset of Figure 3a, is in agreement with the Beer–Lambert law. The dependence of the absorption at 508 nm over iron (iron ions) mass in grams, can be given as A_{508} = 1680 $m(Fe^{2+})$. From Figure 3b and the inset, it can be seen that the maximum absorption that corresponds to the highest iron mass in the solution, was shown in the base coating, followed by that of composite coatings with polyaniline doped with acetic acid, citric acid, succinic acid, and finally sulfamic acid.

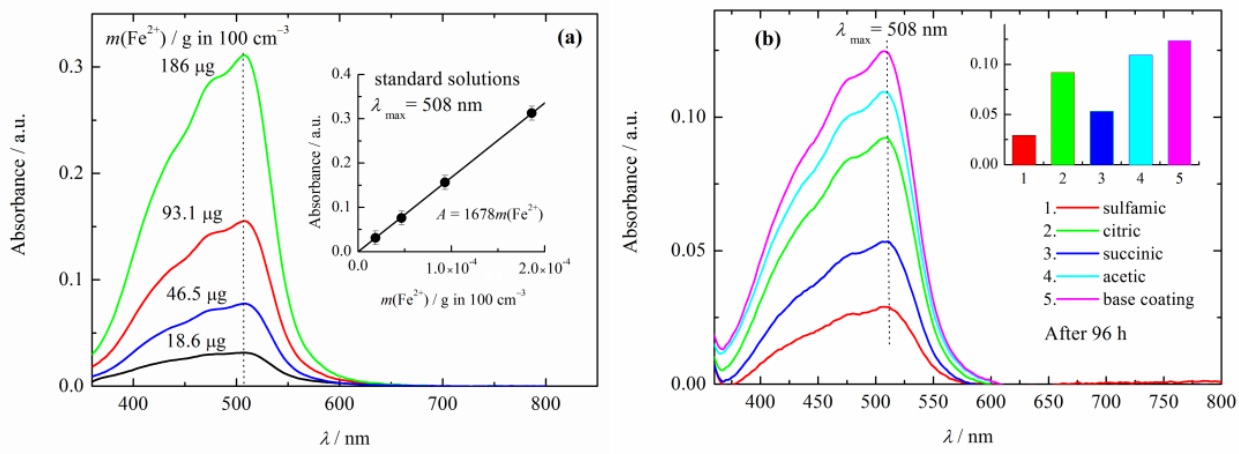

Figure 3. (**a**) UV-vis spectra of the iron standard solutions. Inset: calibration line. (**b**) UV-vis spectra of corrosive solution (3% NaCl) after 96 h of immersions of the composite coatings. Inset: the values of the absorption maximum at 508 nm of the base and composite coatings.

Figure 4 shows the images of the samples before and after immersion in the corrosive media (3% NaCl) for 150 h.

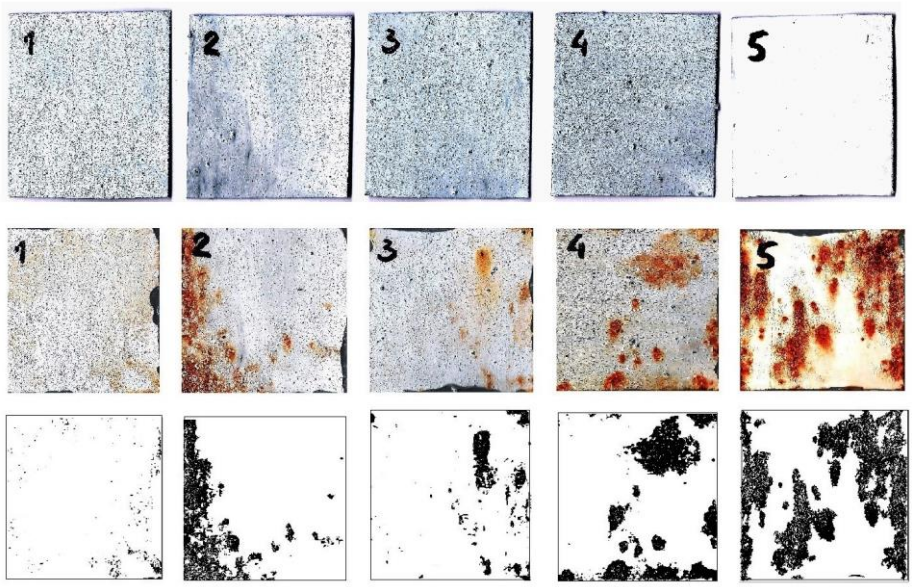

Figure 4. The images of the samples before (**top**), and after immersion in corrosive media (3% NaCl) for 150 h (**middle**). (**bottom**) The images show the visual presentation of the corroded area of the samples as determined by ImageJ software. Composite coatings are marked with 1—sulfamic-acid; 2—citric-acid; 3—succinic-acid, and 4—acetic-acid-doped polyaniline, 5—base coating.

The bottom images show the visual presentation of the corroded area of the samples as determined by ImageJ software, IJ 1.46r, Bethesda, MD, USA. Through visual inspection, it is obvious that the steel sample with the base coating was the most corroded compared to the composite coatings with polyaniline doped with acetic acid, citric acid, succinic acid, and sulfamic acid, which is in agreement with the UV-vis measurements. It should be noted that polyaniline doped with sulfamic acid was practically without any visible corrosion product on its surface.

After exposure to the corrosion media for 150 h, the optical images of the samples with the base coating and composite coatings with polyaniline doped with sulfamic acid were taken and are shown in Figure 5. As can be seen, the base coating was covered with huge blisters, while the composite coating showed only traces of corrosion products. The

other composite coatings showed some corrosion products, Figure 5, but we only observed some small areas of delamination and a few blisters on the composite with PANI doped with acetic acid.

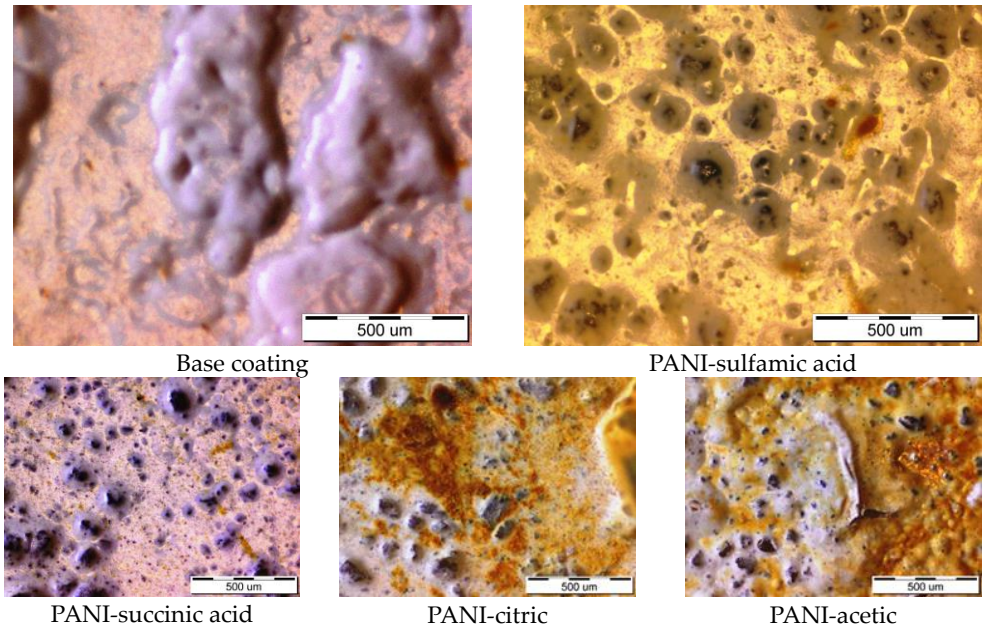

Figure 5. The optical images of the base coating and composite coatings with PANI doped with different organic acids after 150 h of immersion in 3% NaCl.

The main problem with classical organic coatings is the mechanical damage that occurs with rapid corrosion. To investigate the influence of the damage to the coatings, Figure 6 shows the images of the samples before and after 100 h of immersion in 3% NaCl. It is obvious that the sulfamic acid-doped PANI composite coating showed only a trace of corrosion that could be attributed to self-healing properties.

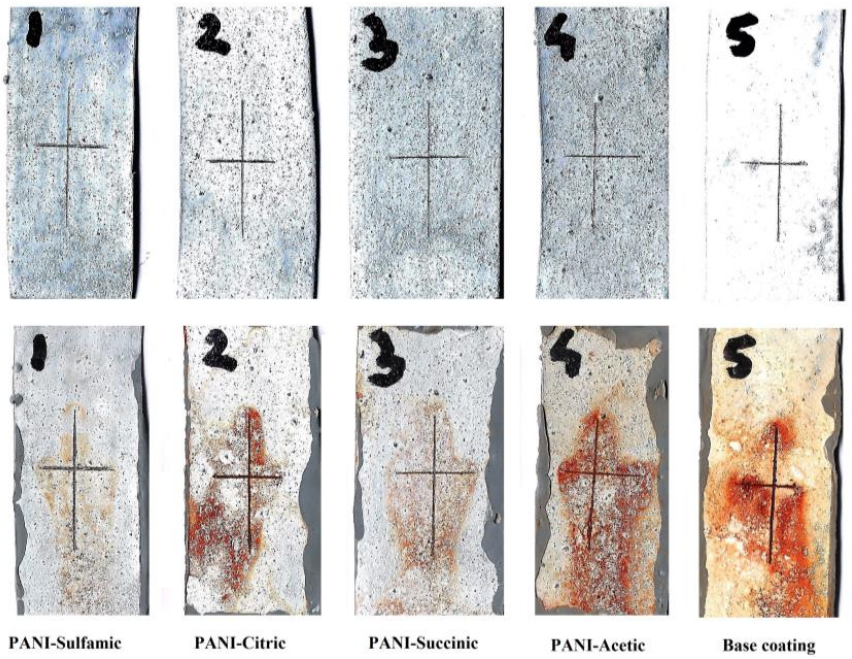

Figure 6. The optical images of the damaged base coating and composite coatings with PANI doped with different organic acids after 100 h of immersion in 3% NaCl.

4. Discussion

Protonated polyaniline can theoretically exist in three fundamental forms: fully reduced leucoemeraldine, half-oxidized emeraldine, and fully oxidized pernigraniline. Of these three forms, only emeraldine salt is conductive [34]. The doping degree, y, represents the average number of doped anions per polymer unit in the polymer chain. For example, emeraldine salt has four monomers in the polymer units and two anions (Scheme 1) so the doping degree is 0.5. Taking into account that PANI prepared following the IUPAC procedure has a doping degree of 0.5, the ratio of absorbance at 440 nm and 365 nm, denoted as $A_{440/365}$ and equal to 1.02, can be used to estimate the doping degrees of the reprotonated samples using the following equation:

$$y = \frac{(A_{440/365}) \times 0.5}{1.02} \quad (1)$$

The determined average doping degrees of the reprotonated samples are shown in Figure 7. It can be seen that sulfamic-acid-doped PANI had an average doping degree of 0.27, PANI–succinic acid was 0.18, PANI–citric acid was 0.15, and PANI–acetic acid was 0.13.

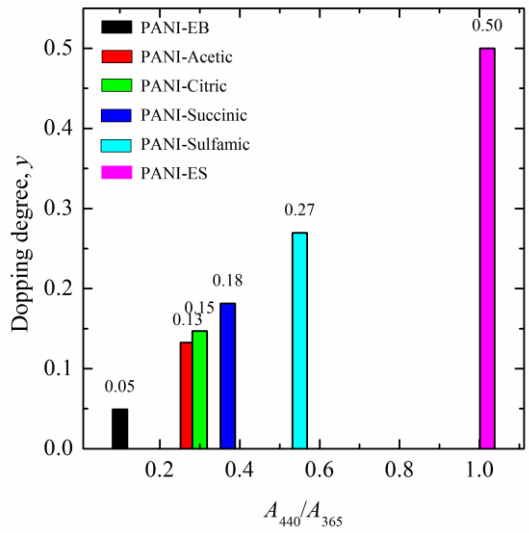

Figure 7. The estimated average doping degrees of the reprotonated PANI samples.

To determine the corrosion rates of the base and composite coatings from the absorbance determined after 96 h of exposure to the corrosive solution, taking into account the calibration curve $A = 1680\ m(Fe^{2+})$, and knowing that the analysis was performed on 10 cm^3 of the corrosive media from 200 cm^3, the average corrosion current density was calculated using the modified equation of the Faraday law:

$$j_{corr} = \frac{A_{508} \times 20 \times n \times F}{1680 \times S \times t \times M(Fe)} \quad (2)$$

where A_{508} is the absorbance at 508 nm after immersion; S, cm^2, is the surface area of the samples; $F = 26.8$ A h mol^{-1} is the Faraday constant; 20 is the conversion factor from 10 cm^3 to 200 cm^3; and M(Fe) is the atomic mass of iron, 55.85 g mol^{-1}. The calculated corrosion current densities are shown in Figure 8a. It is obvious that corrosion current density closely followed the initial doping degree, and decreased with an increase in the initial doping degree. In order to compare the values of the polarization resistance with the determined j_{corr}, Figure 8a shows the data of the reciprocal values of the polarization resistance after 96 h, estimated from Figure 4a in [20]. It should be noted that the thickness of composite coatings for R_p was 40 µm, while for in situ determination it was 25 µm. Because j_{corr} is proportional to ${R_p}^{-1}$, an excellent agreement of the trends of these variables was obtained

using those two methods. Figure 8b shows the comparison of the corrosion current density with the determined corroded surface area after prolonged immersion in 3% NaCl for 150 h (obtained using ImageJ software and shown in Figure 4). The close connections between the initial doping degree, j_{corr}, and appearance of the rust on the sample surfaces are obvious. For example, the base coating surface was covered with 20% rust, while the composite coating with PANI–sulfamic acid was only covered with approximately 1%. Therefore, all of the investigations suggest that the initial PANI doping degree in the composite coatings has a great influence on the corrosion protection behavior on mild steel.

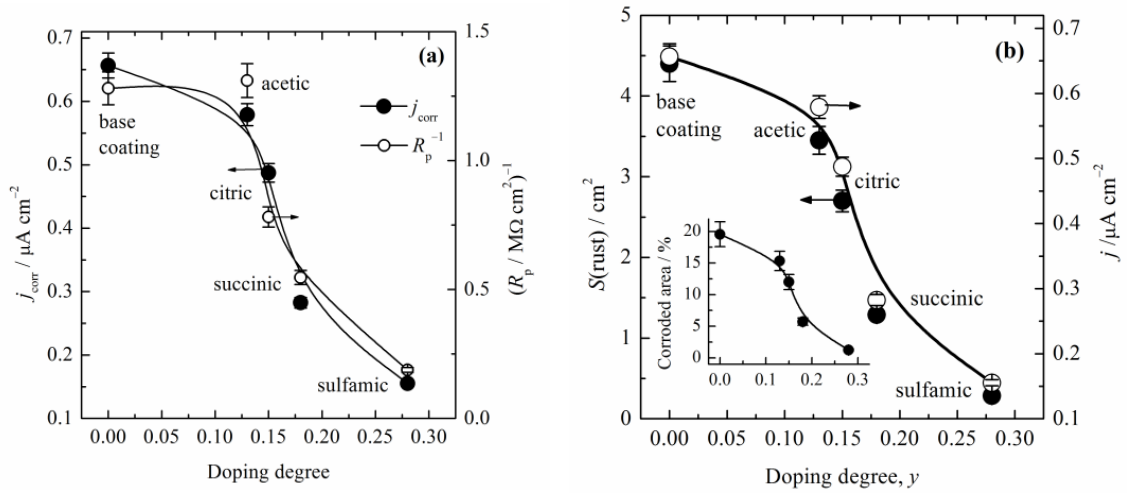

Figure 8. (**a**) The dependence of the calculated corrosion current density and reciprocal values of polarization resistance estimated from [20] vs. doping degree. (**b**) The dependence of the calculated corrosion current density and surface area of the rust formed on the surface of the samples after 150 h of corrosion vs. the doping degree. Inset: The percentage of the corroded area of the samples vs. the doping degree. The size of the symbols represents the experimental error.

The main degradation mechanisms of the base organic coating were delamination and the formation of blisters, as schematically shown in Figure 9 [3,20]. During the immersion in corrosive media, the development of pores in the coating occurs. Blister formation occurred when oxygen and water penetrate through the coating. Oxygen is reduced to OH^- and, with dissolved iron, forms rust that lifts the coatings from the steel surface, as schematically shown in Figure 9a. In the case of delamination (Figure 9b) in two neighboring pores, iron is dissolved in one pore and the released electrons are transferred through the metal to another pore where the oxygen reduction reaction occurs producing OH^- anions; rapid alkalization of the pore occurs, reaching a high pH of 12–13 and, in some cases, more than 14 [35,36], which induces loss of the coating adhesion.

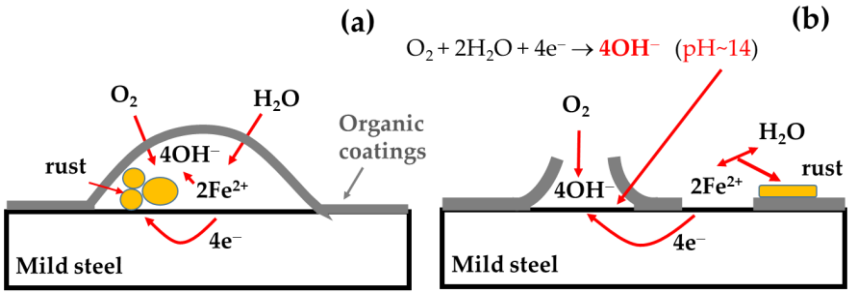

Figure 9. Schematic representations of the organic coating blister formation (**a**) and delamination (**b**).

Polyaniline and polypyrrole have been shown to reduce oxygen to hydrogen peroxide and/or hydroxyl anions via two- or four-electron paths [37–39]. Hereafter, it can be

suggested that polyaniline with a higher doping degree and higher conductivity could reduce oxygen to mainly hydrogen peroxide anions, HO_2^-, lowering the possibility of pH increase and formation of blisters or delamination. By decreasing the doping degree, the conductivity of PANI also decreases, and parallel two and four oxygen reduction paths could occur, but with a much lower concentration of OH^- and a smaller tendency of coating degradation, as schematically presented in Figure 10. It should be also mentioned that the formed hydrogen peroxide anions could react with Fe^{2+} to form a passive film of Fe_2O_3 via the reaction:

$$Fe^{2+} + HO_2^- + H_2O \rightarrow Fe_2O_3 + 3H^+ \quad (3)$$

and immediate reaction:

$$H^- + OH^- \rightarrow H_2O \quad (4)$$

that again lowers the concentrations of OH^- ions in the coating pores. Also, the barrier effect on oxygen penetration due to the presence of the polyaniline particles in the composite coating should be taken into account.

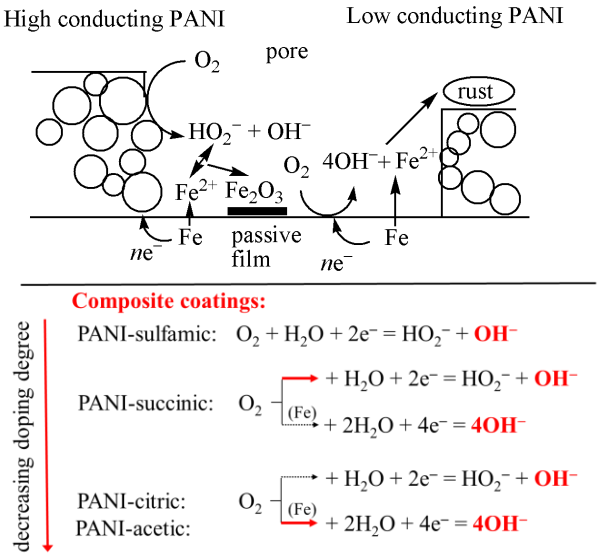

Figure 10. Simplified, schematic representation of the possible reactions during the corrosion of mild steel with composite polyaniline-based coatings. Red arrows represent the main reactions.

Before the conclusions, we can suggest some possible applications of the results from the present study. As shown here and earlier, in addition to solutions of sodium chloride [21,40], polyaniline could protect mild steel in different environments including sand and wet air [41]. From reference [20] it could be concluded that the composite coatings in 3% NaCl could offer a minimum of two to three times longer corrosion protection before deterioration, and probably longer in less aggressive media, especially with their self-healing properties. Unfortunately, due to the agglomeration of the polyaniline particles, the appearance of the coating is not useable finishing paints. Hence, the present formulations with composite coatings could be used as a primer paint for robust steel constructions, like bridges, wagons, reservoirs, trucks, industrial machinery, etc. More efforts should be invested to minimize agglomeration of the polyaniline particles, for example, by the functionalization of the aniline monomers, using water-based paints, and other approaches.

5. Conclusions

- In this paper, we investigated the synthesis of polyaniline in the emeraldine salt form using the procedure suggested by IUPAC.
- The emeraldine salt form was deprotonated with ammonium hydroxide and reprotonated with four different organic acids.

- Using UV–visible spectroscopy, the doping degree was estimated.
- The corrosion performances of the base coating and composite coatings with 5 wt.% of polyaniline doped with organic acids on mild steel were investigated through in situ measurements of iron concentrations in the corrosive media using the ASTM 1,10-phenanthroline method and the corrosion current density was recalculated.
- It was also shown that the protective ability of the composite coatings closely followed the initial oxidation state of the polyaniline, and that polyaniline doped with sulfamic acid with a doping degree of 0.27 had the best corrosion protection ability.
- The damaged composite coatings possessed self-healing properties.
- Blister formation and delamination were suppressed in the composite coatings due to the changes in the oxygen reduction path from the four- to mainly two-electron path, and lowering the concentration of OH^- ions in the pores.

Author Contributions: Conceptualization, funding, methodology, supervision, writing—original draft, writing—review and editing, B.N.G.; investigation, data curation, formal analysis, writing—original draft preparation, A.S.P. and A.S. All authors have read and agreed to the published version of the manuscript.

Funding: This work was supported by the Ministry of Science, Technological Development and Innovation of the Republic of Serbia (Contract No. 451-03-47/2023-01/200135).

Data Availability Statement: Data will be available on request.

Conflicts of Interest: The authors declare that they have no known competing financial interest or personal relationships that could have appeared to influence the work reported in this paper.

References

1. Touileb, K.; Djoudjou, R.; Hedhibi, A.C.; Ouis, A.; Benselama, A.; Ibrahim, A.; Abdo, H.S.; Samad, U.A. Comparative microstructural, mechanical and corrosion study between dissimilar ATIG and conventional TIG weldments of 316L stainless steel and mild steel. *Metals* **2022**, *12*, 635. [CrossRef]
2. Ruan, X.; Yang, L.; Wang, Y.; Dong, Y.; Xu, D.; Zhang, M. Biofilm-induced corrosion inhibition of Q235 carbon steel by *Tenacibaculum mesophilum* D-6 and *Bacillus* sp. Y-6. *Metals* **2023**, *13*, 649. [CrossRef]
3. Lyon, S.B.; Bingham, R.; Mills, D.J. Advances in corrosion protection by organic coatings: What we know and what we would like to know. *Prog. Org. Coat.* **2017**, *102*, 2–7. [CrossRef]
4. Rangel-Olivares, F.R.; Arce-Estrada, E.M.; Cabrera-Sierra, R. Synthesis and characterization of polyaniline-based polymer nanocomposites as anti-corrosion coatings. *Coatings* **2021**, *11*, 653. [CrossRef]
5. Ćirić-Marjanović, G. Recent advances in polyaniline research: Polymerization mechanisms, structural aspects, properties and applications. *Synth. Met.* **2013**, *177*, 1–47. [CrossRef]
6. Ćirić-Marjanović, G. Recent advances in polyaniline composites with metals, metalloids and nonmetals. *Synth. Met.* **2013**, *170*, 31. [CrossRef]
7. Gao, F.; Mu, J.; Bi, Z.; Wang, S.; Li, Z. Recent advances of polyaniline composites in anticorrosive coatings: A review. *Prog. Org. Coat.* **2021**, *151*, 106071. [CrossRef]
8. Hu, C.; Li, T.; Yin, H.; Hu, L.; Tang, J.; Ren, K. Preparation and corrosion protection of three different acids doped polyaniline/epoxy resin composite coatings on carbon steel. *Colloids Surf. A Physicochem. Eng. Asp.* **2021**, *612*, 126069. [CrossRef]
9. Zhang, Y.J.; Shao, Y.W.; Liu, X.L.; Shi, C.; Wang, Y.Q.; Meng, G.Z.; Zeng, X.G.; Yang, Y. A study on corrosion protection of different polyaniline coatings for mild steel. *Prog. Org. Coat.* **2017**, *111*, 240. [CrossRef]
10. Liu, S.; Liu, L.; Meng, F.; Li, Y.; Wang, F. Protective performance of polyaniline-sulfosalicylic acid/epoxy coating for 5083 aluminum. *Materials* **2018**, *11*, 292. [CrossRef]
11. Zhang, Y.; Shao, Y.; Zhang, T.; Meng, G.; Wang, F. The effect of epoxy coating containing emeraldine base and hydrofluoric acid doped polyaniline on the corrosion protection of AZ91D magnesium alloy. *Corros. Sci.* **2011**, *53*, 3747–3755. [CrossRef]
12. Baloch, A.; Kannan, M.B. Electropolymerisation of aniline on AZ91 magnesium alloy: The effect of coating electrolyte corrosiveness. *Metals* **2017**, *7*, 533. [CrossRef]
13. Ma, Y.; Fan, B.; Liu, H.; Fan, G.; Hao, H.; Yang, B. Enhanced corrosion inhibition of aniline derivatives electropolymerized coatings on copper: Preparation, characterization and mechanism modeling. *Appl. Surf. Sci.* **2020**, *514*, 146086. [CrossRef]
14. Xu, H.; Zhang, Y. A review on conducting polymers and nanopolymer composite coatings for steel corrosion protection. *Coatings* **2019**, *9*, 807. [CrossRef]
15. Armelin, E.; Alemán, C.; Iribarren, J.I. Anti-corrosion performances of epoxy coatings modified with polyaniline: A comparison between the emeraldine base and salt forms. *Prog. Org. Coat.* **2009**, *65*, 88. [CrossRef]

16. Diniz, F.B.; De Andrade, G.F.; Martins, C.R.; De Azevedo, W.M. A comparative study of epoxy and polyurethane based coatings containing polyaniline-DBSA pigments for corrosion protection on mild steel. *Prog. Org. Coat.* **2013**, *76*, 912. [CrossRef]
17. Kohl, M.; Kalendová, A. Effect of polyaniline salts on the mechanical and corrosion properties of organic protective coatings. *Prog. Org. Coat.* **2015**, *86*, 96. [CrossRef]
18. Liu, T.; Wei, J.; Ma, L.; Liu, S.; Zhang, D.; Zhao, H. Effect of polyaniline-based plate on the anticorrosion performance of epoxy coating. *Prog. Org. Coat.* **2021**, *151*, 106109. [CrossRef]
19. Kumar, A. Role of conducting polymers in corrosion protection. *World J. Adv. Res. Rev.* **2023**, *17*, 45–47. [CrossRef]
20. Salem, A.J.; Grgur, B.N. The influence of the polyaniline initial oxidation states on the corrosion of steel with composite coatings. *Prog. Org. Coat.* **2018**, *119*, 138. [CrossRef]
21. Salem, A.J.; Grgur, B.N. Corrosion of mild steel with composite alkyd polyaniline-benzoate coating. *Int. J. Electrochem. Sci.* **2017**, *12*, 8683. [CrossRef]
22. Stejskal, J.; Gilbert, R.G. Polyaniline: Preparation of a conducting polymer (IUPAC Technical Report). *Pure Appl. Chem.* **2002**, *74*, 857. [CrossRef]
23. Stejskal, J.; Prokeš, J.; Trchová, M. Reprotonation of polyaniline: A route to various conducting polymer materials. *React. Funct. Polym.* **2008**, *68*, 1355. [CrossRef]
24. *E 394–00*; Standard Test Method for Iron in Trace Quantities Using the 1,10-Phenanthroline Method. ASTM: West Conshohocken, PA, USA, 2000.
25. Available online: https://imagej.nih.gov/ij/docs/guide/user-guide.pdf (accessed on 6 June 2023).
26. Jin, E.; Liu, N.; Lu, X.; Zhang, W. Novel micro/nanostructures of polyaniline in the presence of different amino acids via a self-assembly process. *Chem. Lett.* **2007**, *36*, 1288. [CrossRef]
27. de Albuquerque, J.E.; Mattoso, L.H.C.; Faria, R.M.; Masters, J.G.; MacDiarmid, A.G. Study of the interconversion of polyaniline oxidation states by optical absorption spectroscopy. *Synth. Met.* **2004**, *146*, 1–10. [CrossRef]
28. Sk, M.M.; Yue, C.Y. Synthesis of polyaniline nanotubes using the self-assembly behavior of vitamin C: A mechanistic study and application in electrochemical supercapacitors. *J. Mater. Chem. A* **2014**, *2*, 2830. [CrossRef]
29. Han, Y.-G.; Kusunose, T.; Sekino, T. One-step reverse micelle polymerization of organic dispersible polyaniline nanoparticles. *Synth. Met.* **2009**, *159*, 123. [CrossRef]
30. Wang, X.; Li, Y.; Zhao, Y.; Liu, J.; Tang, S.; Feng, W. Synthesis of PANI nanostructures with various morphologies from fibers to micromats to disks doped with salicylic acid. *Synth. Met.* **2010**, *160*, 2008. [CrossRef]
31. Prevost, V.; Petit, A.; Pla, F. Studies on chemical oxidative copolymerization of aniline and o-alkoxysulfonated anilines: I. Synthesis and characterization of novel self-doped polyanilines. *Synth. Met.* **1999**, *104*, 79. [CrossRef]
32. Xia, H.; Wang, Q. Synthesis and characterization of conductive polyaniline nanoparticles through ultrasonic assisted inverse microemulsion polymerization. *J. Nanopart. Res.* **2001**, *3*, 401. [CrossRef]
33. Bertuoli, P.T.; Baldissera, A.F.; Zattera, A.J.; Ferreira, C.A.; Alemán, C.; Armelin, E. Polyaniline coated core-shell polyacrylates: Control of film formation and coating application for corrosion protection. *Prog. Org. Coat.* **2019**, *128*, 40. [CrossRef]
34. Beygisangchin, M.; Abdul Rashid, S.; Shafie, S.; Sadrolhosseini, A.R.; Lim, H.N. Preparations, properties, and applications of polyaniline and polyaniline thin films—A Review. *Polymers* **2021**, *13*, 2003. [CrossRef]
35. Leidheiser, H.; Wang, W.; Igetoft, L. The mechanism for the cathodic delamination of organic coatings from a metal surface. *Prog. Org. Coat.* **1983**, *11*, 19. [CrossRef]
36. Tator, K.B. Coating deterioration, ASM handbook. In *Protective Organic Coatings*; Tator, K.B., Ed.; ASM International: Amir, The Netherlands, 2015; Volume 5B, pp. 462–473.
37. Rabl, H.; Wielend, D.; Tekoglu, S.; Seelajaroen, H.; Neugebauer, H.; Heitzmann, N.; Apaydin, D.H.; Scharber, M.C.; Sariciftci, N.S. Are polyaniline and polypyrrole electrocatalysts for oxygen (O_2) reduction to hydrogen peroxide (H_2O_2)? *ACS Appl. Energy Mater.* **2020**, *3*, 10611. [CrossRef]
38. Grgur, B.N. Metal | polypyrrole battery with the air regenerated positive electrode. *J. Power Sources* **2014**, *272*, 1053. [CrossRef]
39. Khomenko, V.G.; Barsukov, V.Z.; Katashinskii, A.S. The catalytic activity of conducting polymers toward oxygen reduction. *Electrochim. Acta* **2005**, *50*, 1675. [CrossRef]
40. Grgur, B.N.; Elkais, A.R.; Gvozdenović, M.M.; Drmanić, S.Ž.; Trišović, T.L.j.; Jugović, B.Z. Corrosion of mild steel with composite polyaniline coatings using different formulations. *Prog. Org. Coat.* **2015**, *79*, 17. [CrossRef]
41. Elkais, A.R.; Gvozdenović, M.M.; Jugović, B.Z.; Grgur, B.N. The influence of thin benzoate-doped polyaniline coatings on corrosion protection of mild steel in different environments. *Prog. Org. Coat.* **2013**, *76*, 670. [CrossRef]